

Dynamics of the Functional Activity and Expression of Proteasome Subunits during Cellular Adaptation to Heat Shock

A. V. Morozov^{a,*}, A. V. Burov^{a,b}, T. M. Astakhova^c, D. S. Spasskaya^a, B. A. Margulis^d, and V. L. Karpov^a

^aEngelhardt Institute of Molecular Biology, Russian Academy of Sciences, Moscow, 119991 Russia

^bFaculty of Biology, Moscow State University, Moscow, 119991 Russia

^cKoltsov Institute of Developmental Biology, Russian Academy of Sciences, Moscow, 119334 Russia

^dInstitute of Cytology, Russian Academy of Sciences, St. Petersburg, 194064 Russia

*e-mail: Runkel@inbox.ru

Received November 6, 2018; revised November 26, 2018; accepted November 26, 2018

Abstract—The ubiquitin-proteasome system (UPS) performs proteolysis of most intracellular proteins. The key components of the UPS are the proteasomes, multi-subunit protein complexes, playing an important role in cellular adaptation to various types of stress. We analyzed the dynamics of the proteasome activity, the content of proteasome subunits, and the expression levels of genes encoding catalytic subunits of proteasomes in the human histiocytic lymphoma U937 cell line immediately, 2, 4, 6, 9, 24, and 48 h after a heat shock (HS). The initial decrease (up to 62%) in the proteasome activity in cellular lysates was revealed, then 10 h after HS the activity began to recover. The amount of proteasomal α -subunits in the cells decreased 2 h after HS, and was restored to 24–48 h after HS. Fluctuations in the levels of mRNAs encoding proteasome catalytic subunits with the maximum expression 2 h after HS and a gradual decrease to 48 h after HS were observed. The average estimated number of mRNA copies per cell ranged from 10 for weakly to 150 for highly expressed proteasome genes. Thus, the recovery efficiency of UPS functionality after HS, which reflects the important role of proteasomes in maintaining cell homeostasis, was evaluated.

Keywords: ubiquitin-proteasome system, proteasome, heat shock

DOI: 10.1134/S0026893319040071

INTRODUCTION

The ubiquitin-proteasome system (UPS) degrades most intracellular proteins and, thus, participates in almost all basic metabolic processes and in maintaining cell homeostasis [1]. The core element of the UPS is the 20S proteasome, a barrel-like structure composed of four rings made of seven subunits each. Each of the two outer rings consists of seven α -subunits ($\alpha 1$ – 7) and performs structural and protective functions, preventing the unregulated access of substrates to the catalytic chamber formed by the two rings of β -subunits. Three of the seven β -subunits in each ring are catalytically active and perform the hydrolysis of polypeptide chains after acidic ($\beta 1$), basic ($\beta 2$), and hydrophobic ($\beta 5$) amino acid residues [2]. Furthermore, instead of the constitutive subunits, proteasomes may contain so-called immune subunits ($\beta 1i$, $\beta 2i$, and $\beta 5i$), the expression of which is stimulated by different cytokines (interferon- γ (IFN γ) and tumor necrosis factor- α (TNF α)) and increases with oxidative stress [3]. The 20S proteasome performs its functions in cells either in its free form or in complexes with

regulators, generating different forms of proteasomes [4, 5]. The regulators ensure the substrate specificity of proteasomes and facilitate the substrate penetration, thus affecting the proteasomal activity. The main parameter characterizing the functional state of proteasomes is their catalytic activity.

Proteasomes play a key role in protecting a cell from different stresses. Thus, the proteasome-dependent degradation of oxidized and damaged proteins helps the cells to cope with oxidative stress [6]. Damaged protein species are actively accumulated under the stress caused by elevated ambient temperatures. Although the UPS state after a heat shock (HS) was investigated in a number of works [7–9], changes in the proteasome activity and proteasome cellular levels after HS were insufficiently addressed. In this work, the functional state of proteasomes in the human histiocytic lymphoma U937 cell line was studied before and within 48 h after HS.

EXPERIMENTAL

Cells. The human histiocytic lymphoma U937 cell line (courtesy of V.S. Prasolov, Engelhardt Institute of

Abbreviations: UPS, ubiquitin-proteasome system, HS, heat shock.

Molecular Biology, Russian Academy of Sciences) was cultured in the RPMI 1640 medium (Gibco, United Kingdom) supplemented with 10% fetal bovine serum (FBS) (HyClone, United Kingdom), 2 mM *L*-glutamine, and antibiotics (penicillin/streptomycin) at 37°C, 5% CO₂, and 95% humidity.

Heat shock. Before being exposed to HS, the U937 cells were counted in a Goryaev chamber and collected in separate test tubes (1×10^6 cells per tube). The test tubes were placed in a water bath (43°C) and incubated for 1 h. After incubation, the cells were transferred into culture flasks, placed in an incubator, and maintained at 37°C, 5% CO₂, and 95% humidity. Before the exposure to HS, immediately after HS, and 2, 4, 6, 9, 24, and 48 h after HS, the cells were harvested by centrifugation, counted in a Goryaev chamber, and washed with phosphate buffer (PB). Afterwards, the cells were either frozen at -80°C (for the proteasome activity assay or RNA isolation) or lysed in a buffer [50 mM Tris-HCl (pH 8.0), 150 mM NaCl, 1% NP-40, 5 mM EDTA, a protease inhibitor cocktail (Complete mini EDTA free (Roche, Switzerland))] at the ratio of 1 µL of the buffer per 10⁴ cells. Nuclear and cytoplasmic extracts were obtained with the NE-PER Nuclear and cytoplasmic extraction reagent kit (Thermo Scientific, United States) according to the manufacturer's instructions.

Assessment of proteasome activity. The chymotrypsin-like activity of proteasomes in cell homogenates was assessed as described earlier [10]. The cells were thawed and homogenized in the ratio of 1×10^6 cells per 70 µL of the homogenization buffer [50 mM Tris-HCl (pH 7.5), 100 mM NaCl, 5 mM MgCl₂, 1 mM EDTA, 1 mM dithiothreitol, 10% glycerol, 10 mM Na₂S₂O₅, and 2 mM ATP]. Total protein content in the samples was determined using the Lowry method [11]. The chymotrypsin-like activity of proteasomes was determined by the hydrolysis of fluorogenic substrate Suc-LLVY-AMC (Sigma-Aldrich, United States) on a VersaFluor Fluorometer (Bio-Rad, United States). The activity assays were carried out in triplicates, in 100 µL of a buffer for the activity assay, containing 6 µL of clarified homogenate [12]. To control the proteasome-related specific activity, it was also determined in the samples containing the homogenate and added 10 µM of the proteasome inhibitor MG132 (Sigma-Aldrich, United States). The obtained values were recalculated for 1 µL of the clarified homogenate, multiplied by the normalizing factor (obtained after estimation of the protein content in the samples). The mean value and standard deviation were calculated; then the content (%) was recalculated relative to the activity in the control cells.

Inhibitory analysis and western blotting. The dynamics of the proteasome concentration after HS were also evaluated in lysates of the cells treated with inhibitors of proteasomal and lysosomal proteolysis. Before HS, the inhibitors (either a proteasome inhibi-

tor MG132 (Sigma-Aldrich) at a concentration of 5 µM or a lysosomal proteolysis inhibitor chloroquine (Sigma-Aldrich) at a concentration of 10 µM) were added to the cell culture medium. Afterwards, the culture medium was exposed to HS and subsequent manipulations as described above.

The subunit composition of proteasomes in cell lysates was analyzed by Western blot. Proteins were separated with electrophoresis in a 12% denaturing polyacrylamide gel (PAAG) containing sodium dodecyl sulfate (SDS) in a Tris-glycine buffer and then transferred onto the nitrocellulose membrane (Bio-Rad, United States). To monitor the transfer efficiency, the membranes were stained with a 0.1% Ponceau Rouge solution (Sigma-Aldrich). To identify proteasome subunits, the membranes were incubated with primary antibodies (Table 1) for 2 h, then washed with PBS containing 0.1% Tween 20 (Fisher Scientific, United States), and incubated with appropriate horseradish peroxidase-conjugated (HRP) secondary antibodies (Table 1). The blots were developed using the ECL Prime kit (GE Healthcare, UK). To normalize the signal, the membranes were washed from the antibodies, at first, with an antibody removal buffer (PBS, 2% SDS, 100 mM β-mercaptoethanol), and then additionally with PBS. The membranes were incubated with primary antibodies against β-actin (Table 1), then washed, and incubated with appropriate secondary HRP-labeled antibodies (Table 1) and developed as described above.

Ultracentrifugation. The secretion of proteasomes via extracellular vesicles (EVs) from the cells exposed to HS was assessed. For this purpose, the cell culture medium was replaced with the fresh one, and then cells were exposed to HS. The cell culture medium was collected (immediately after HS, as well as 2, 4, 6, 9, 24, and 48 h after HS), centrifuged at 400 g for 5 min, and then at 5000 g for 5 min. The supernatant was collected after each centrifugation, transferred into a new tube, and the pellets were discarded. The obtained samples were centrifuged (100000 g, 2 h) through a 10% sucrose solution in a Beckman Ultima ultracentrifuge (Beckman, United States). The pellets were dissolved in PBS and analyzed with immunoblotting as described above.

Development of a real-time PCR (RT-qPCR) system. From the cells exposed to HS and frozen at -80°C, the total RNA was isolated using the GeneJET RNA Purification Kit (Thermo Scientific) according to the manufacturer's instructions. The RNA concentration and purity in the samples were determined spectrophotometrically with a NanoDrop instrument (Thermo Scientific). To remove DNA, the RNA samples were treated with the RapidOut DNA Removal kit (Thermo Scientific). Further, a reverse transcription reaction was performed using Maxima H Minus Reverse Transcriptase (Thermo Scientific) and an oligo(dT)₂₀ primer to obtain cDNA (1.5 µg of the total

Table 1. Antibodies used in the study

Antibodies	Manufacturer
Mouse monoclonal anti-20S proteasome α -subunits (α 1,2,3,5,6,7)	Enzo, United States
Rabbit polyclonal anti- β 5	GeneTex, United States
Rabbit monoclonal anti- β 5i	Cell signaling, United States
Rabbit polyclonal anti-Hsp70	Courtesy of M.B. Evgen'ev
Mouse monoclonal anti-Rpt6 (Rpt6 subunit of 19S-regulator)	Enzo, United States
Rabbit monoclonal anti- β -actin	Sigma-Aldrich, United States
Goat anti-mouse IgG (HRP)	Enzo, United States
Goat polyclonal anti-rabbit IgG (HRP)	Abcam, UK

RNA in the reaction mixture). The expression level of genes encoding proteasome catalytic subunits (*PSMB5*, *PSMB6*, *PSMB7*, *PSMB8*, *PSMB9*, and *PSMB10*), as well as β -actin (*Actb*) and heat shock protein 70 (Hsp70, *HSPA1A* gene), was quantified by the RT-qPCR assay. Primers for PCR (Table 2) were selected using the IDT platform (<https://eu.idtdna.com>) and the OligoAnalyzer tool, considering the criteria described in [13]. With these primers, the PCR products were obtained. After purification from agarose gel, the PCR products were cloned (except for *HSPA1A*) into the pAL-2T vector, using the Quick TA kit (Evrogen, Russia). Thus, a set of plasmids with short gene fragments corresponding to the PCR products was obtained. The plasmids concentrations were measured utilizing the NanoDrop instrument (Thermo Scientific). Using the EndMemo online tool (<http://www.endmemo.com/bio/dnacopynum.php>), we determined the copy number of each plasmid per unit volume. At the next stage, the PCR amplification efficiency of specific fragments was assessed. Serial dilutions of plasmids were applied as a template. The PCR products were separated on a 2.5% agarose gel (see Supplementary Materials, Fig. 1). In the tests, we determined the reaction optimal parameters and the system sensitivity. Then, the amplification efficiency of each primer pair was estimated by qPCR using the Luminaris Color HiGreen qPCR Master Mix kit (Thermo Scientific) and serial dilutions of plasmids and serial dilutions of cDNA (see Supplementary Materials, Figs. 2, 3). Reactions with control plasmids were carried out in the presence of 100 ng of carrier DNA (salmon sperm DNA (Thermo Scientific)). At the stage of applying the designed RT-qPCR system for quantification of expression levels of genes encoding proteasome catalytic subunits, 2 μ L of 4 times diluted cDNA was added per each reaction. Each experimental point (C, 0, 2, 4, 6, 9, 24, and 48 h) for all genes was performed in duplicate, and the system calibration was carried out with serial dilutions of plasmids (2, 10, 10^2 , 10^3 , 10^4 , 10^6 , and 10^7 copies of each plasmid was added to the reaction). The qPCR was performed on a LightCycler 480 instrument (Roche). The output data of the instrument, including the val-

ues of the threshold cycles, were analyzed with Microsoft Excel tools. Based on the obtained calibration curves (the values of the threshold cycles for serial dilutions of an appropriate plasmid), the number of transcripts of each gene per unit volume were determined. Further, the number of transcripts per μ g of the total RNA was calculated, and afterwards, the average number of gene transcripts per cell was estimated. For this purpose, it was necessary to estimate the average amount of total RNA per cell. Therefore, an additional experiment was carried out. RNA was isolated in triplicate from a known number of cells and the RNA concentration was measured. The mean RNA abundance per cell of the U937 line was 12 ± 1 pg. This value was used in estimating the number of each gene transcripts per cell. The expression level was normalized to *Actb*.

RESULTS AND DISCUSSION

Dynamics of Proteasome Activity in U937 Cells after HS

A sharp decrease in the proteasome activity in HS-exposed U937 cells was demonstrated (Fig. 1). Thus, immediately after HS, the chymotrypsin-like activity of proteasomes reached 70% of the initial value, and

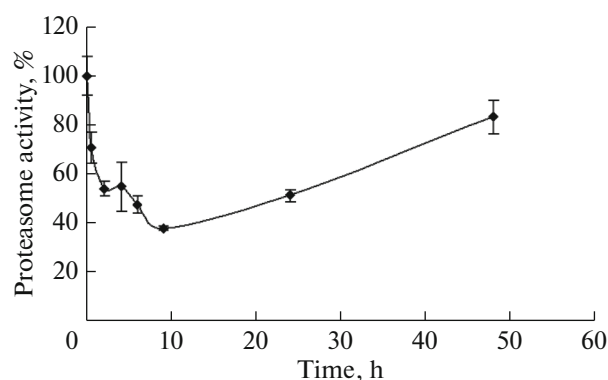


Fig. 1. Dynamics of chymotrypsin-like activity of proteasomes in lysates of U937 cells after HS. Proteasome activity was determined by hydrolysis of fluorogenic Suc-LLVY-AMC substrate. Experiment was carried out in three replications.

Table 2. Primers used in the study

Primer	Nucleotide sequence 5' → 3'	Length, bp	Location as per reference mRNA	Amplicon length, bp	Thermodynamic parameters*		
					T_m , °C	Homodimers and hairpins, min ΔG , kcal/mol	Heterodimers, min ΔG , kcal/mol
PSMB5 fw	CTCCAAACTGCTTGCCAAC	19	NM_002797.4 bp 678–696	Exon–exon, 121	61.9	–3.9	–3.29
PSMB5 rev	GTTCCCTTCACTGTCCACG	19	NM_002797.4 bp 798–780		62.5	–3.61	
PSMB6 fw	AAGCCGAGAAAGTTTCCACT	19	NM_002798.2 bp 132–150	Exon–exon, 102	61.7	–3.61	–4.64
PSMB6 rev	GCGATGTAGACCCAGT	17	NM_002798.2 bp 233–217		60.7	–3.61	
PSMB7 fw	CTGAAAGGGATGGTTGTTG	18	NM_002799.3 bp 239–256	Exon–exon, 128	58	–1.94	–3.55
PSMB7 rev	CAGGTTGGAAGAAATGAGC	19	NM_002799.3 bp 366–348		58.8	–3.14	
PSMB8 fw	GGTGAACAAGGTGATTGAG	19	NM_148919.3 bp 349–367	Exon–exon, 128	58.5	–3.9	–4.86
PSMB8 rev	GTTCTCCATTTCCGAGATAG	20	NM_148919.3 bp 476–457		58.5	–3.61	
PSMB9 fw	GCTGCTGATGCCCAAGC	17	NM_002800.4 bp 274–290	Exon–exon, 117	63.9	–4.74	–4.74
PSMB9 rev	GCTGATAATTTCTCACCA-CATTTC	24	NM_002800.4 bp 390–367		62.9	–3.91	
PSMB10 fw	GGTTCCAGCCGAACATGA	18	NM_002801.3 bp 667–684	Exon–exon, 106	62.2	–5.38	–3.61
PSMB10 rev	ATGCGTCCACATTGCCCC	17	NM_002801.3 bp 772–756		63.1	–3.61	
Actb fw	TTGGCAATGAGCGGTTCC	18	NM_001101.4 bp 941–958	Exon–exon, 93	63.2	–3.9	–3.9
Actb rev	GAGTTGAAGGTAGTTTCGTGG	21	NM_001101.4 bp 1033–1014		60.8	–3.61	
Hsp70 fw	GAGTCCTACGCCCTTCAACAT	20	NM_005345.5 bp 1870–1980	The same exon, 110	61.9	–3.61	–5.47
Hsp70 rev	CGAGATGACCTCTTGACACTT	21			61.8	–3.61	
T7 Primer	TAATACGACTCACTATAGGG	20			55.5	–6.59	

* Thermodynamic parameters of primers were evaluated with IDT OligoAnalyzer Tool (<https://eu.idtdna.com/pages>) at following salt content: $[Na^+]$, 50 mM; $[Mg^{2+}]$, 3 mM; and $[dNTP]$, 0.8 mM.

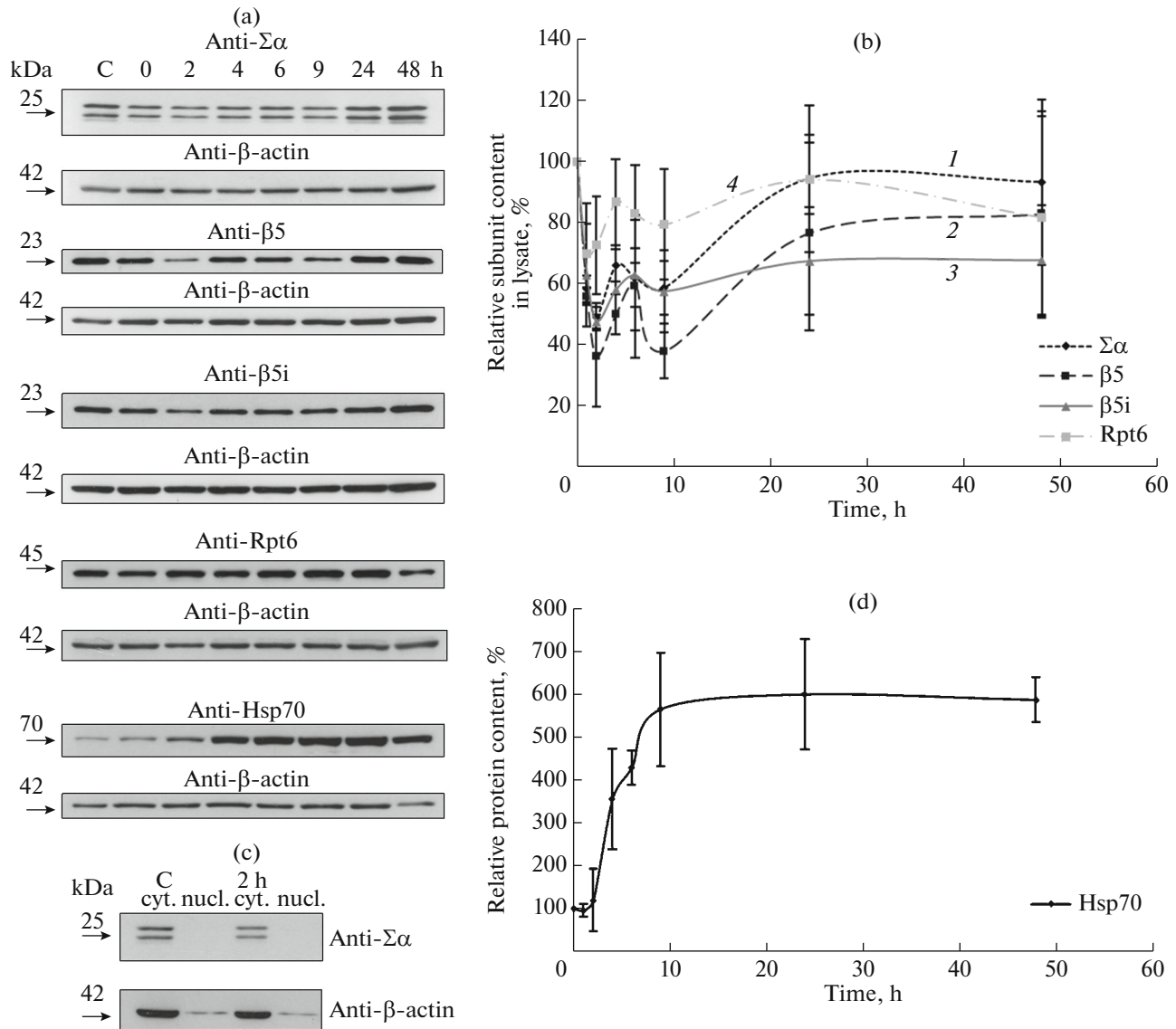


Fig. 2. Analysis of proteasome subunit level in U937 cells after HS. (a) Western blot of lysates of control cells and of cells incubated for 0, 2, 4, 6, 9, 24, and 48 h after HS with antibodies against proteasome subunits, 19S regulator subunit Rpt6, and Hsp70. At least two biological replicates were performed, in experiment to study dynamics of content of proteasomal α -subunits, $n = 4$. Representative results are presented for each experiment. (b) Changes in levels of proteasome subunits and proteasome regulator after HS. Graph is plotted based on average optical density of relevant signals obtained after scanning X-ray films and processing results with ImageJ software. Mean optical density value in control is denoted as 100%. Curves: (1) $\Sigma\alpha$; (2) $\beta 5$; (3) $\beta 5i$; and (4) Rpt6. (c) Comparative analysis of content of proteasomal α -subunits in lysates of cytoplasmic and nuclear fractions of control cells and U937 cells 2 h after HS. (d) Accumulation of Hsp70 in U937 cells after HS. Graph is plotted based on average optical density of relevant signals obtained after scanning X-ray films and processing results with ImageJ software. Mean optical density value in control is denoted as 100%.

2 h after HS, it was 54%. The lowest proteasome activity level in U937 lysates (38% of the initial level) was observed 9 h after HS (Fig. 1). Then the activity was gradually restored to approximately 85% of the control level 48 h after HS. The experimental results indicating a decrease in the proteasome activity coincide with the previous measurements of the proteasome activity 2 h after HS (in RMA cells, 25 min, 42°C) [7]. At the same time, the proteasome activity profile, deter-

mined by us, differed from the data obtained in human fibroblasts after they were exposed to HS (for 1 h at 41 or 42°C) [8]. Thus, 5 h after HS, the chymotrypsin-like activity of proteasomes decreased by approximately 14% [8], followed by its sharp growth. However, the data [8] demonstrate a more significant decrease in the proteasome activity in the cells exposed to HS at higher temperatures (for example, at 43°C) [8]. Thus, we can see similar dynamics in the

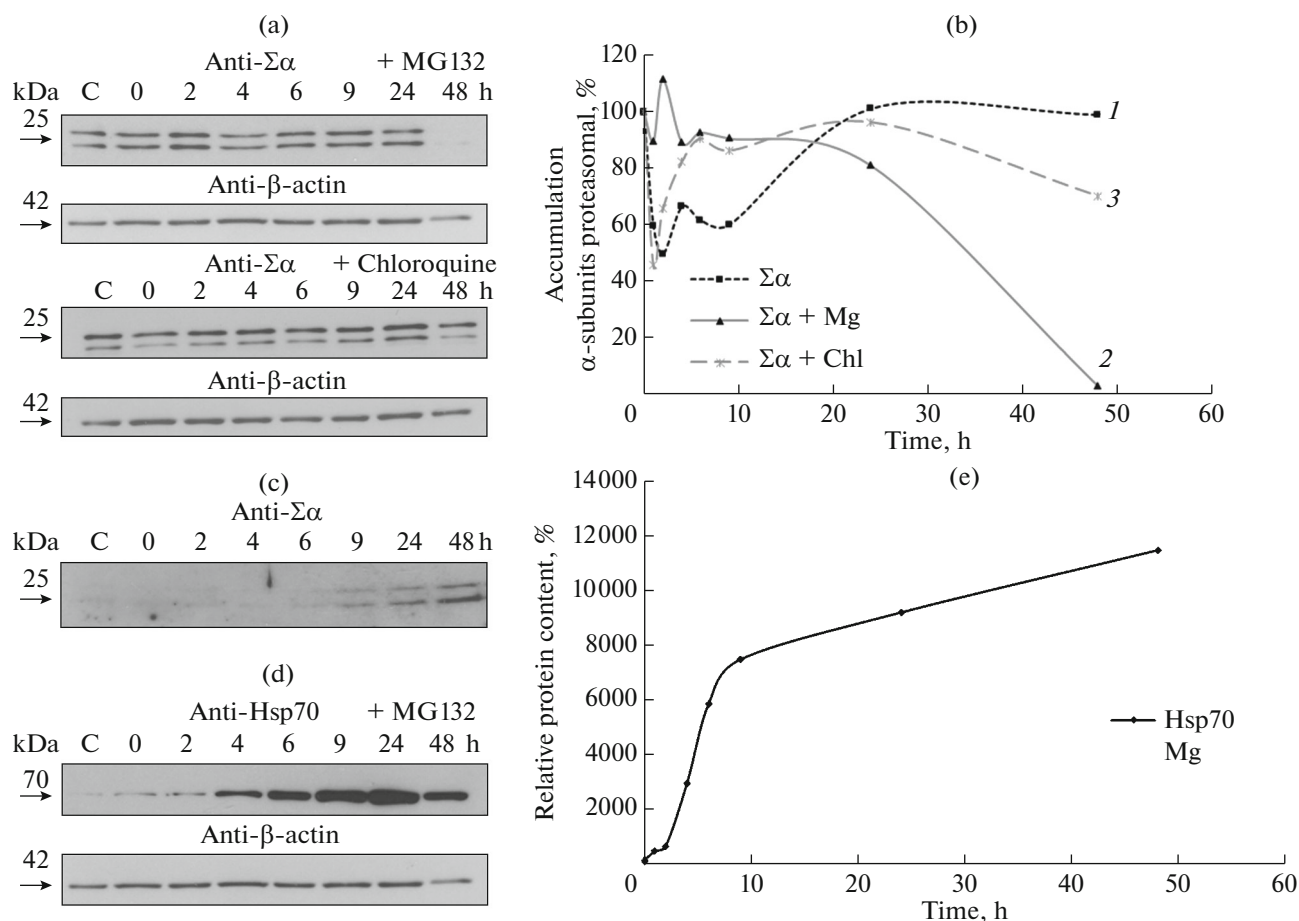


Fig. 3. Effects of MG132 proteasome inhibitor and lysosomal proteolysis inhibitor chloroquine on accumulation dynamics of proteasomal α -subunits in cellular lysates of U937 after HS. (a) Western blot of cellular lysates with antibodies against proteasomal α -subunits. Cells were exposed to HS in presence of inhibitors, and then cellular lysates were obtained immediately after HS, as well as 2, 4, 6, 9, 24, and 48 h after HS. (b) Changes in content of proteasome α -subunits after HS in presence of inhibitors (Mg—MG132, Chl—chloroquine). Graph is plotted based on average optical density of relevant signals obtained after scanning X-ray films and processing results with ImageJ software. Mean optical density value in control is denoted as 100%. Curves: (1) $\Sigma\alpha$; (2) $\Sigma\alpha + \text{MG132}$; and (3) $\Sigma\alpha + \text{Chloroquine}$. (c) Western blot of samples of culture fluid of U937 cells (100 times concentrated by ultracentrifugation) obtained at different intervals after HS. Each sample (20 μL) was applied on gel. (d) Western blot analysis of lysates of U937 cells after HS in presence of proteasome inhibitor MG132 with antibodies against Hsp70. (e) Accumulation of Hsp70 in U937 cells after HS in presence of proteasome inhibitor MG132. Graph is plotted based on average optical density of relevant signals obtained after scanning X-ray films and processing results with ImageJ software. Mean optical density value in control is denoted as 100%.

response of different cells to elevated temperature, although the dynamics of proteasome activity seem to be strongly dependent on the HS protocol and type of cells. Possible reasons of the decline in the activity may include less efficient proteasome maturation, post-translational modifications (PTMs) of their subunits [7], and a decreased abundance of the existing assembled complexes. Therefore, we have investigated the dynamics of the abundance of proteasome subunits in cellular lysates after HS.

Dynamics of Proteasome Subunit and Hsp70 Levels in U937 Lysates after HS

The proteasome content in cellular lysates was assessed by Western blot with antibodies to the struc-

tural α -subunits ($\alpha 1, 2, 3, 5, 6, 7$) and to the catalytic subunits $\beta 5$ and $\beta 5i$ responsible for the chymotrypsin-like activity of proteasomes. In addition, the content of Rpt6 subunit of the 19S proteasome regulator was determined. The amounts of the proteasome subunits in cellular lysates began to decrease immediately after HS and reached their minimum 2 h after HS (Figs. 2a, 2b). Afterwards, the content of proteasome subunits and subunits of the 19S regulator was restored. However, the abundance of proteasomes recovered unevenly. Thus, the subunit levels increased within 2–6 h after HS, followed by stabilization or decreasing by the 9th h after HS, with the further recovery of the proteasome abundance (Figs. 2a, 2b). Considering our method of preparation of cell lysates (gentle lysis without disrupting the cell nuclei) and the data

reported in [7] indicating changes in the intracellular localization of proteasomes after HS, we compared the proteasome content in the nuclear and cytoplasmic fractions prepared from the control cells and from the cells incubated within 2 h after HS (Fig. 2c). No significant increase in the proteasome levels in the nuclei lysates was revealed. Moreover, in the nuclear fraction of U937 cells, proteasome α -subunits were practically absent. These results are consistent with the recently published results, indicating a predominantly cytoplasmic localization of the active proteasomes, at least in some cell lines [14]. Although the data on the decrease in the proteasome abundance differ from those presented earlier [8], these differences may be a result of using different cell lines and different HS protocols. As an additional control, we assessed the level of Hsp70 in U937 lysates. It began to grow sharply 2–4 h after HS and reached a peak around 9 h, then the protein level stabilized and remained at the same level even 48 h after HS (Figs. 2a, 2d).

Effects of Proteasome and Lysosome Inhibitors on the Cellular Proteasome Levels after HS

Under stress conditions, proteasomes are degraded by autophagy [15, 16]. It is known that exposure to HS (43°C) increases autophagy, and the autophagy markers LC3I and LC3II are accumulated within 3–6 h after HS [17]. To estimate the autophagy contribution to the observed decrease in the proteasome subunit content in U937 lysates, HS was performed in the presence of a lysosomal proteolysis inhibitor, chloroquine. It was shown that in the presence of chloroquine, the recovery of cellular proteasome subunit levels occurs faster (Figs. 3a, 3b). The amount of proteasome subunits in lysates of the cells incubated with chloroquine barely decreased 6 and 9 h after HS, which might indicate that part of the proteasomes are degraded in autophagosomes 6–9 h after HS; this, however, does not fully explain the decrease in the proteasome subunit level 2–4 h after HS (Figs. 3a, 3b). It is known that proteasomes could be secreted from the cells within the extracellular vesicles (EVs) both under normal and stress conditions [18, 19]. Therefore, we evaluated the possible release of proteasomes from the cells via exosomes or microvesicles after HS. Ultracentrifugation of the cell culture fluid samples revealed a gradually increasing abundance of the encapsulated α -subunits of the proteasomes. This indicates the likely absence of any rapid release of proteasomes via EVs immediately after HS (Fig. 3c).

It can be assumed that the proteasome subunits not incorporated into the proteasomes can be degraded by other proteasomes. It was shown that subunit Rpn5 of regulator 19S was degraded in yeast cells [20]. It is also known that most of the proteasome subunits are actively ubiquitinated, and at least some of them undergo this modification without being incorporated in the complex [21]. Although proteasomal subunits

are mainly monoubiquitinated, it was recently shown that this might be quite sufficient for the substrate degradation in proteasomes [22]. Furthermore, HS induces the active degradation of de novo synthesized proteins [23]. In our studies, we observed stabilization in the level of proteasome α -subunits in lysates in the presence of the MG132 proteasome inhibitor 2 h after HS. This may be indicative of the degradation of unassembled proteasome subunits in functionally active proteasomes or indicate the disruption of mechanisms involved in the degradation of proteasomes themselves. The latter seems less likely, since the proteasome subunit levels still continue to decrease when the autophagy is inhibited (Figs. 3a, 3b). At the same time, a sharp decrease in the proteasome abundance observed 24 h after HS may be a result of the autophagy activation due to the inhibition of proteasomes [24]. The Hsp70 accumulation in cellular lysates was more pronounced in the presence of MG132 (Figs. 3d, 3e). However, the most significant increase of the protein content began 4 h after HS (similarly to the experiments without the inhibitor). These data show the joint effect of the proteasome inhibition and HS, which coincides with the previously reported results [25–27].

Dynamics of the Proteasome Subunit Genes mRNA Levels after HS

Using the designed RT-PCR system for quantification of the expression levels of proteasome genes, we estimated the accumulation of specific transcripts in the cells after HS. We determined the mRNA levels of the *PSMB5*, *PSMB6*, *PSMB7*, *PSMB8*, *PSMB9*, and *PSMB10* genes encoding the subunits $\beta 5$, $\beta 1$, $\beta 2$, $\beta 5i$, $\beta 1i$, and $\beta 2i$, respectively, and the expression level of the *HSPA1A* gene. It was shown that, normally, the number of transcripts of the proteasome genes in the U937 cells varies from 10 (*PSMB9* and *PSMB10* genes) to about 120 (*PSMB8*) copies per cell (Fig. 4). These data demonstrate the heterogeneity of the proteasome pool in U937 cells and the prevalence of intermediate proteasomes containing the set of catalytic subunits $\beta 1$, $\beta 2$, $\beta 5i$, which is in good agreement with the results of the mass spectrometric analysis [28]. Immediately after HS the decrease in the mRNA levels of genes encoding the constitutive proteasome subunits ($\beta 1$, $\beta 2$, $\beta 5$) was observed. Two hours after HS, the number of specific transcripts increased, and, afterwards, decreased. However, 9 h after HS, it began to grow again, approaching the values measured before exposure to HS. The increased transcript levels 2 h after HS could explain the increase in the concentration of proteasomal subunits 4 h after HS, as revealed earlier (Figs. 2a, 2b). In the case of the immune subunit genes *PSMB8* and *PSMB10* the dynamics of mRNA expression was different. Thus, after a peak 2 h after HS, a smooth decline during subsequent 46 h was observed. These data may, to some extent, explain the extremely slow elevation of the $\beta 5i$ subunit level (Figs. 2a, 2b). In general, the

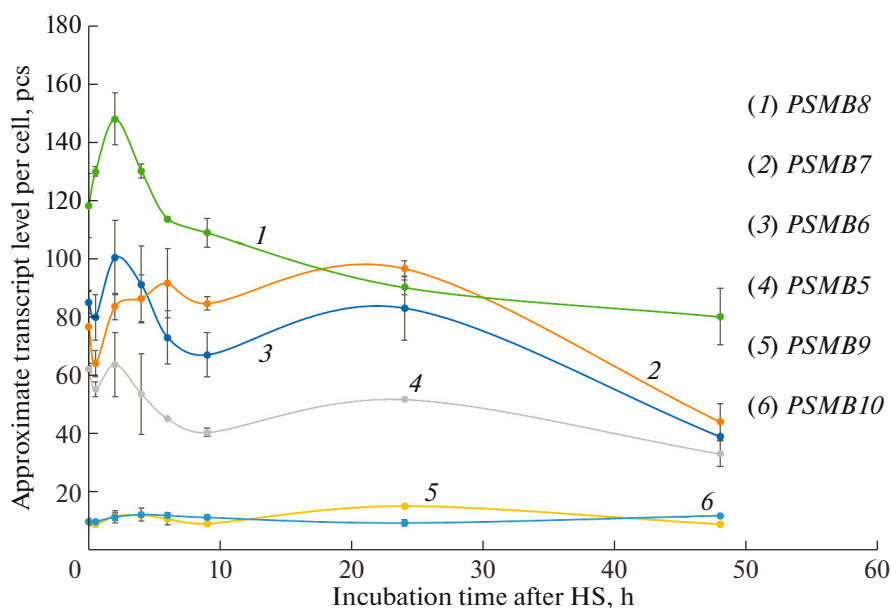


Fig. 4. Accumulation of mRNAs of proteasomal genes in U937 cells after HS quantified by RT-qPCR.

results of the experiments demonstrate changes in the cellular proteasome pool and likely increased share of constitutive proteasomes 24 h after HS. The expression level of gene encoding Hsp70 was represented by a peak with a maximum 9 h after HS, when the estimated mRNA copy number per cell reached about 8.000 and then it promptly decreased, and after 48 hours, it approached the control values (see Supplementary Materials, Fig. 4). It should be noted that the evaluated transcripts levels per cell are approximate values, since the RNA isolation efficacy or the efficiency and processivity of the reverse transcriptase were not considered.

CONCLUSIONS

Additional data on the complex nature of the UPS adaptation to HS were obtained. Changes in the functional activity of proteasomes after HS are apparently due to the action of a whole set of factors, including changes in the expression level of subunits, degradation of proteasomes and their subunits, disruption in the assembly of complexes, and the PTMs of proteasome subunits. Considering the important role of proteasomes in maintaining homeostasis in normal cells and, especially, in tumor cells, and the development of methods for thermal tumor ablation [29], the studies on molecular mechanisms of the UPS adaptation to HS are capable of providing the necessary information for modifying the protocols for cancer therapy.

ACKNOWLEDGMENTS

The authors thank V.A. Morozov for participating in the discussion of the results.

FUNDING

An RT-PCR system for the quantification of the expression levels of proteasome genes was designed, tested, and tuned with the financial support of the Russian Science Foundation (grant no. 18-74-10095). The studies on the proteasomal activity and their subunit composition in lysates of U937 cells were supported by the grant of the President of the Russian Federation for young PhD scientists (grant no. MK3613.2017.4) and financially supported under the Program of Fundamental Research of the State Academies of Sciences for 2013–2020, subject no. 01201363823.

COMPLIANCE WITH ETHICAL STANDARDS

Conflict of interest. The authors declare that they have no conflict of interest.

Statement of the welfare of animals. This article does not contain any studies involving animals or human participants performed by any of the authors.

SUPPLEMENTARY MATERIALS

Supplementary materials are available for this article at <https://doi.org/10.1134/S0026893319040071> and are accessible for authorized users.

REFERENCES

- Goldberg A.L. 2007. Functions of the proteasome: From protein degradation and immune surveillance to cancer therapy. *Biochem. Soc. Trans.* **35**, 12–17.
- Livneh I., Cohen-Kaplan V., Cohen-Rosenzweig C., Avni N., Ciechanover A. 2016. The life cycle of the 26S proteasome: From birth, through regulation and function, and onto its death. *Cell Res.* **26**, 869–885.

3. Pickering A.M., Linder R.A., Zhang H., Forman H.J., Davies K.J. 2012. Nrf2-dependent induction of proteasome and Pa28alpha-beta regulator are required for adaptation to oxidative stress. *J. Biol. Chem.* **287**, 10021–10031.
4. Fort P., Kajava A.V., Delsuc F., Coux O. 2015. Evolution of proteasome regulators in eukaryotes. *Genome Biol. Evol.* **7**, 1363–1379.
5. Morozov A.V., Karpov V.L. 2018. Biological consequences of structural and functional proteasome diversity. *Heliyon.* **4**, e00894.
6. Pickering A.M., Koop A.L., Teoh C.Y., Ermak G., Grune T., Davies K.J. 2010. The immunoproteasome, the 20S proteasome and the PA28alpha-beta proteasome regulator are oxidative-stress-adaptive proteolytic complexes. *Biochem. J.* **432**, 585–594.
7. Kuckelkorn U., Knuehl C., Boes-Fabian B., Drung I., Kloetzel P.M. 2000. The effect of heat shock on 20S/26S proteasomes. *Biol. Chem.* **381**, 1017–1023.
8. Kraft D.C., Deocaris C.C., Rattan S.I. 2006. Proteasomal oscillation during mild heat shock in aging human skin fibroblasts. *Ann. N.Y. Acad. Sci.* **1067**, 224–227.
9. Kim H.J., Joo H.J., Kim Y.H., Ahn S., Chang J., Hwang K.B., Lee D.H., Lee K.J. 2011. Systemic analysis of heat shock response induced by heat shock and a proteasome inhibitor MG132. *PLoS One.* **6**, e20252.
10. Morozov A.V., Yurinskaya M.M., Mit'kevich V.A., Garbuz D.G., Preobrazhenskaya O.V., Vinokurov M.G., Evgen'ev M.B., Karpov V.L., Makarov A.A. 2017. Heat-shock protein HSP70 decreases activity of proteasomes in human neuroblastoma cells treated by amyloid-beta 1-42 with isomerized Asp7. *Mol. Biol. (Moscow)* **51** (1), 166–171.
11. Lowry O.H., Rosebrough N.J., Farr A.L., Randall R.J. 1951. Protein measurement with the Folin phenol reagent. *J. Biol. Chem.* **193**, 265–275.
12. Karpova Ya.D., Lyupina Yu.V., Astakhova T.M., Stepanova A.A., Erokhov P.A., Abramova E.B., Sharova N.P. 2013. Immune proteasomes in the development of the rat immune system. *Russ. J. Bioorg. Chem.* **39** (4), 356–365.
13. Morozov V.A., Morozov A.V., Denner J. 2016. New PCR diagnostic systems for the detection and quantification of porcine cytomegalovirus (PCMV). *Arch. Virol.* **161**, 1159–1168.
14. Dang F.W., Chen L., Madura K. 2016. Catalytically active proteasomes function predominantly in the cytosol. *J. Biol. Chem.* **291**, 18765–18777.
15. Cohen-Kaplan V., Livneh I., Avni N., Fabre B., Ziv T., Kwon Y.T., Ciechanover A. 2016. p62- and ubiquitin-dependent stress-induced autophagy of the mammalian 26S proteasome. *Proc. Natl. Acad. Sci. U. S. A.* **113**, E7490–E7499.
16. Cuervo A.M., Palmer A., Rivett A.J., Knecht E. 1995. Degradation of proteasomes by lysosomes in rat liver. *Eur. J. Biochem.* **227**, 792–800.
17. Zhao Y., Gong S., Shunmei E., Zou J. 2009. Induction of macroautophagy by heat. *Mol. Biol. Rep.* **36**, 2323–2337.
18. Bochmann I., Ebstein F., Lehmann A., Wohlschlaeger J., Sixt S.U., Kloetzel P.M., Dahlmann B. 2014. T lymphocytes export proteasomes by way of microparticles: A possible mechanism for generation of extracellular proteasomes. *J. Cell. Mol. Med.* **18**, 59–68.
19. Tucher C., Bode K., Schiller P., Classen L., Birr C., Souto-Carneiro M.M., Blank N., Lorenz H.M., Schiller M. 2018. Extracellular vesicle subtypes released from activated or apoptotic T-lymphocytes carry a specific and stimulus-dependent protein cargo. *Front. Immunol.* **9**, 534.
20. Peters L.Z., Karmon O., David-Kadoch G., Hazan R., Yu T., Glickman M.H., Ben-Aroya S. 2015. The protein quality control machinery regulates its misassembled proteasome subunits. *PLoS Genet.* **11**, e1005178.
21. Moiseeva T.N., Bottrill A., Melino G., Barlev N.A. 2013. DNA damage-induced ubiquitylation of proteasome controls its proteolytic activity. *Oncotarget.* **4**, 1338–1348.
22. Braten O., Livneh I., Ziv T., Admon A., Kehat I., Caspi L.H., Gonen H., Bercovich B., Godzik A., Jahandideh S., Jaroszewski L., Sommer T., Kwon Y.T., Guharoy M., Tompa P., Ciechanover A. 2016. Numerous proteins with unique characteristics are degraded by the 26S proteasome following monoubiquitination. *Proc. Natl. Acad. Sci. U. S. A.* **113**, E4639–4647.
23. Medicherla B., Goldberg A.L. 2008. Heat shock and oxygen radicals stimulate ubiquitin-dependent degradation mainly of newly synthesized proteins. *J. Cell Biol.* **182**, 663–673.
24. Sha Z., Schnell H.M., Ruoff K., Goldberg A. 2018. Rapid induction of p62 and GABARAP1 upon proteasome inhibition promotes survival before autophagy activation. *J. Cell Biol.* **217**, 1757–1776.
25. Grossin L., Etienne S., Gaborit N., Pinzano A., Cournil-Henrionnet C., Gerard C., Payan E., Netter P., Terlain B., Gillet P. 2004. Induction of heat shock protein 70 (Hsp70) by proteasome inhibitor MG 132 protects articular chondrocytes from cellular death in vitro and in vivo. *Biorheology.* **41**, 521–534.
26. Mathew A., Mathur S.K., Morimoto R.I. 1998. Heat shock response and protein degradation: Regulation of HSF2 by the ubiquitin-proteasome pathway. *Mol. Cell. Biol.* **18**, 5091–5098.
27. Bush K.T., Goldberg A.L., Nigam S.K. 1997. Proteasome inhibition leads to a heat-shock response, induction of endoplasmic reticulum chaperones, and thermotolerance. *J. Biol. Chem.* **272**, 9086–9092.
28. Fabre B., Lambour T., Garrigues L., Ducoux-Petit M., Amalric F., Monsarrat B., Burlet-Schiltz O., Bousquet-Dubouch M.P. 2014. Label-free quantitative proteomics reveals the dynamics of proteasome complexes composition and stoichiometry in a wide range of human cell lines. *J. Proteome Res.* **13**, 3027–3037.
29. Chu K.F., Dupuy D.E. 2014. Thermal ablation of tumours: Biological mechanisms and advances in therapy. *Nat. Rev. Cancer.* **14**, 199–208.

Translated by M. Romanova